Nature of the divergence in low shear viscosity of colloidal hard-sphere dispersions

Zhengdong Cheng, Jixiang Zhu, and Paul M. Chaikin
Department of Physics, Princeton University, Princeton, New Jersey 08544

See-Eng Phan and William B. Russel
Department of Chemical Engineering, Princeton Materials Institute, Princeton University, Princeton, New Jersey 08544

(Received 11 November 2001; published 8 April 2002)

Measurements of the low-shear viscosity η_o with a Zimm-Crothers viscometer for dispersions of colloidal hard spheres are reported as a function of volume fraction ϕ up to 0.56. Nonequilibrium theories based on solutions to the two-particle Smoluchoski equation or ideal mode coupling approximations do not capture the divergence. However, the nonhydrodynamic contribution to the relative viscosity $\Delta\eta_o$ is correlated over a wide range of volume fractions by the Doolittle and Adam-Gibbs equations, indicating an exponential divergence at $\phi_m = 0.625 \pm 0.015$. The data extend the previously proposed master curve, providing a test for improved theories for the many-body thermodynamic and hydrodynamic interactions that determine the viscosity of hard-sphere dispersions.

DOI: 10.1103/PhysRevE.65.041405 PACS number(s): 82.70.Dd, 83.80.Hj, 83.10.Tv

I. INTRODUCTION

The next step beyond the ideal gas is the hard sphere, which captures excluded volume interactions in atomic or colloidal systems but still ignores attractions. These produce an entropy-driven disorder-order transition with liquid and crystal coexisting for volume fractions ϕ between freezing $\phi_f = 0.494$ and melting $\phi_m = 0.545$ [1] and a dynamic glass transition at a higher volume fraction $\phi_g = 0.56-0.58$ [2]. The hard-sphere fluid provides a reference system for the study of molecular and colloidal fluids [3], so insight into the metastable fluid and glass should contribute to understanding of the glass transition phenomena more broadly.

Several model colloidal suspensions, such as poly(methyl methacrylate) (PMMA) spheres with a grafted layer of poly(12-hydroxy stearic acid) (PHSA) [4] or bare silica particles [5] in a refractive index matched solvent, behave as hard spheres. Earlier studies of dispersions of colloidal hard spheres confirmed the phase diagram [6,7] and the equation of state for the fluid and crystal [8] derived from computer simulations and also determined shear viscosities and viscoelastic moduli for dilute and moderately concentrated dispersions [5,8–13]. Colloidal hard spheres have also been employed in studies of the kinetics of nucleation and growth of the crystalline phase [14] and the lattice dynamics of crystals [15]. Such experiments are easier with colloidal dispersions than with molecular systems because of the much longer length and time scales, which make experimental tools such as laser light scattering and optic microscopy appropriate. For colloids, random Brownian motion on the diffusion time scale is the manifestation of the kinetic energy of the molecules, while the solvent provides a background that transports momentum and modulates the interaction potentials. So colloidal hard spheres have exactly the same phase diagram as a molecular hard sphere. However, the exchange of momentum in dynamic processes is considerably different, since one must deal with many-body hydrodynamic interactions in the colloidal case.

The rheology of colloidal hard spheres has its own importance. Krieger [9] recognized early on that hard spheres provide a baseline or convenient reference for understanding more complicated complex fluids, including many everyday materials of technological importance. Viscosity also serves as a useful indicator for the onset of a glass transition [16]. Finally, data for hard spheres provide an essential test for theories that must approximate many-body thermodynamic and hydrodynamic interactions [17] to predict the rheology of concentrated dispersions.

The stress in dispersions of hard spheres of radius a has contributions from hydrodynamic and thermodynamic, i.e., Brownian and interparticle, forces as defined by Batchelor [18]. In the low shear or weak flow limit the former derives from many-body hydrodynamic interactions among spheres with equilibrium spatial distributions. The contribution to the low-shear viscosity η_o corresponds to that for high-frequency oscillations, denoted by η_∞'. At equilibrium the Brownian and interparticle forces produce only an isotropic structure and stress, i.e., an osmotic pressure. A shear flow perturbs the spatial distribution from the isotropic equilibrium state, generating a deviatoric stress with magnitude for hard spheres proportional to the thermal energy density kT/a^3 times the Brownian relaxation time a^2/D_s^o, with D_s^o the short-time self-diffusion coefficient. Combining these produces a low-shear viscosity of the form

$$\eta_o = \eta_\infty' + \frac{kT}{6\pi D_s^o a}\Delta\eta_o, \tag{1}$$

with $\Delta\eta_o$ representing the dimensionless contribution due to Brownian motion and the interparticle potential. The high-frequency viscosity and the short-time self-diffusion coefficient depend only on hydrodynamic interactions among spheres at equilibrium but differ in the cause of fluid motion, which is an imposed rate of strain for the former and a random force on a single particle in the latter. This fundamental similarity is reflected in the (short time) generalized Stokes-Einstein relation,

$$D_s^o = \frac{kT}{6\pi\eta_\infty' a}\Delta d_s^o. \tag{2}$$

 ©2002 The American Physical Society

For hard spheres, theory and experiments indicate $\Delta d_s^o = 0.5-2.0$ [19] for a wide range of volume fractions, suggesting the approximation

$$\eta_o \cong \eta'_\infty \{1+\Delta\eta_o\}. \tag{3}$$

By analogy to Eq. (2) one can define a generalized (long time) Stokes-Einstein relation between η_o and the long-time self-diffusion coefficient D_s^∞ as

$$D_s^\infty = \frac{kT}{6\pi\eta_0 a}\Delta d_s^\infty, \tag{4}$$

with Δd_s^∞ close to unity for moderate concentrations of hard spheres. Recent measurements and theory indicate, however, that Δd_s^∞ can deviate substantially from unity at high concentrations [16,19].

The ''hydrodynamic rescaling'' approximation (3) has been employed to predict the low-shear viscosity of concentrated dispersions of hard spheres from calculations of $\Delta\eta_o$ for dispersions without hydrodynamic interactions [20] and for molecular hard spheres via mode coupling theory [19], as described below. The analytical approximation for the high-frequency viscosity [21],

$$\frac{\eta'_\infty}{\mu} = \begin{cases} \dfrac{1+\frac{3}{2}\phi[1+\phi(1+\phi-2.3\phi^2)]}{1-\phi[1+\phi(1+\phi-2.3\phi^2)]}, & 0\leqslant\phi\leqslant 0.56, \\ 15.78\ln\dfrac{1}{1-1.160\phi^{1/3}}-42.47, & 0.60\leqslant\phi<0.64 \end{cases} \tag{5}$$

is consistent with the exact dilute limit and results from Stokesian dynamics simulations and experiments on concentrated dispersions. Likewise, the relationship between η_o and D_s^∞ is the basis for phenomenological models for the viscosity of molecular fluids near the glass transition.

II. BACKGROUND

From the colloidal perspective, most approaches have evolved from the derivation of Batchelor [18] of the low-shear viscosity for hard spheres in the dilute or pair interaction limit. The nonequilibrium pair distribution function is extracted from the Smoluchoski equation, which balances diffusion and translation due to the interparticle potential against deformation due to the flow, with hydrodynamic interactions modulating all three fluxes. The thermodynamic stresses follow as integrals of the Brownian and interparticle forces weighted by the pair distribution function and modulated by hydrodynamic mobilities. The resulting virial expansions for the high-frequency viscosity and the thermodynamic contribution,

$$\frac{\eta'_\infty}{\mu} = 1+2.5\phi+5.0\phi^2, \quad \Delta\eta_o = 1.0\phi^2, \tag{6}$$

determine the low-shear viscosity as

$$\frac{\eta_o}{\mu} = 1+2.5\phi+6.0\phi^2. \tag{7}$$

The most popular phenomenological correlation of the low-shear viscosity with volume fraction at higher concentrations, originated by Krieger and Dougherty [9], takes the form of $\eta_o/\mu = (1-\phi/\phi_m)^{-2}$. Recently Brady [20] rescaled the prediction for the low-shear viscosity at infinite dilution without hydrodynamic interactions, obtained by solving the Smoluchoski equation, to account for (a) far-field hydrodynamic interactions via η'_∞ and (b) the larger number of nearest neighbors at finite concentrations through the Percus-Yevick approximation for the radial distribution function at contact $g(2;\phi)$. From this emerged the appealingly simple result

$$\Delta\eta_o = \tfrac{12}{5} g(2;\phi)\phi^2. \tag{8}$$

Since both $\eta'_\infty(5)$ and $g(2;\phi)$ diverge at random close packing as $(\phi_m-\phi)^{-1}$ with $\phi_m = 0.637-0.644$, this provides theoretical support for the Krieger-Dougherty formula. In the dilute limit where $g(2;0)=1$, Eq. (8) leads to an $O(\phi^2)$ term of $7.4\phi^2$.

A variety of more systematic approximations, employing the Smoluchoski equation to determine the nonequilibrium structure and standard expressions for the Brownian and interparticle stresses, have been proposed since Batchelor's exact theory for the dilute limit. Determining the validity, self-consistency, and accuracy has proven difficult or at least contentious. Recently Wagner and co-workers [22] applied the GENERIC algorithm to test the various approaches for thermodynamic self-consistency. Those found to be inconsistent included the simplest, rescaling of the dilute limit to obtain Eq. (8), and the most complex, implementation of a nonequilibrium version of the hypernetted chain closure [17]. The next simplest self-consistent approximation replaces the pair potential in both the Smoluchoski equation and the interparticle stress with the potential of mean force, $\Phi_{\rm mf} = -kT\ln g(r,\phi)$. Of course, this does not imply the closure to be accurate and says nothing about the accompanying hydrodynamic approximation, e.g., rescaling. The resulting predictions of η_o for monodisperse hard spheres diverge, roughly quadratically, at random close packing.

The Stokesian dynamics simulations developed by Brady [23] accurately compute the many-body hydrodynamics forces and incorporate Brownian motion and the hard-sphere excluded volume to generate both equilibrium and nonequilibrium structures, albeit for rather small numbers of particles (generally 27) per periodic box. Use of a Green-Kubo relation eliminates the need to extrapolate the nonequilibrium results to the low-shear limit and provides accurate low-shear viscosities for volume fractions up to 0.49 [24]. In addition, the accurate calculation of hydrodynamic mobilities serves to motivate the hydrodynamic rescaling approximation and validate more sophisticated ones [17]. In this spirit one can rescale recent Brownian dynamics simulations without hydrodynamic interactions and with many more particles (1331–2000) [25] to extend the results to $\phi = 0.55$.

From the molecular perspective the rapid increase in viscosity for fluids approaching the glass transition with either

decreasing temperature or increasing pressure has stimulated numerous phenomenological models that predict $\Delta\eta_o$ [16,26]. Free volume arguments of Cohen and Turnbull [27] focus on the environment surrounding a molecule in a dense fluid and derive the probability for the appearance of sufficiently large cavities for the molecule to diffuse, thereby escaping the ''cage'' of nearest neighbors. This leads to an expression for the diffusion coefficient as $D=a^*\ u\exp(-\gamma\nu^*/\nu_f)$ with u the thermal velocity, a^* a size on the order of a molecular diameter, ν^* the minimum free volume for motion, ν_f the average free volume per molecule, and γ an $O(1)$ constant. Taking the average free volume for hard spheres as $\nu_f/\nu^*=\phi^{-1}-\phi_m^{-1}$, with ϕ_m referring to the Kauzmann volume fraction or random close packing, and the prefactor as $a^*\ u\propto D_s^o$ yields a long-time self-diffusion coefficient of the form $1/D_s^\infty=1/D_s^o+1/\Delta D_s^\infty$ with

$$\Delta D_s^\infty \propto D_s^o \exp\left(-\frac{\gamma\phi\phi_m}{\phi_m-\phi}\right). \tag{9}$$

The derivation then calls on the long-time generalized Stokes-Einstein equation, i.e., Eq. (4) with $\Delta d_s^\infty=1$, to produce the Doolittle equation,

$$\Delta\eta_o = C\exp\left(\frac{\gamma\phi\phi_m}{\phi_m-\phi}\right). \tag{10}$$

C and γ normally are assumed to be constants, though strictly speaking the former should vanish as $\phi\to 0$. As noted earlier, the validity of this approach is somewhat suspect, since Δd_s^∞ tends to depart from unity in the vicinity of the glass transition in molecular systems or close packing for colloidal dispersions.

In contrast to the free volume approach, which focuses on individual particles hopping into free volume to escape their cages, the Adam-Gibbs theory [16] addresses cooperative rearrangements of groups of molecules or particles. As the system approaches the glass transition or close packing, relaxation requires the coordinated motion of progressively larger numbers of particles z^*. The analysis expresses the size of the region, $z^*=s_{\rm conf}^*/S_{\rm conf}$, in terms of the configurational entropy $S_{\rm conf}$ in the excess of that associated with local motions that do not alter the nearest neighbors of a particle. The long-time self-diffusion coefficient follows as

$$D\propto \exp\left(-\frac{s_{\rm conf}^*\delta\mu}{S_{\rm conf}kT}\right), \tag{11}$$

with $s_{\rm conf}^*=O(k\ln 2)$ the entropy of the minimum number of particles and $\delta\mu$ the chemical potential barrier to motion. Translating this into colloidal terms and invoking the long-time Stokes-Einstein equation, as for the free volume approach, suggests

$$\Delta\eta_o \cong C\exp\left(\frac{\delta\mu\ln 2}{TS_{\rm conf}}\right), \tag{12}$$

with C and $\delta\mu$ the unknown parameters. The configurational entropy for hard spheres can be derived from the total entropy,

$$TS=-\int^{\phi} Z(\phi)\frac{d\phi}{\phi} \tag{13}$$

with $Z(\phi)$ the compressibility factor, as $S_{\rm conf}=S-\lim_{\phi\to\phi_m} S$. Here we take $Z(\phi)$ from the Carnahan-Starling equation for the equilibrium fluid up to $\phi=0.49$ and employ an analytical fit to recent simulations [28] for $0.49<\phi<\phi_m=0.644$. As $\phi\to\phi_m\ S_{\rm conf}\sim(\phi_m-\phi)$, so the Adam-Gibbs prediction for the viscosity should asymptote to that from the Doolittle equation.

Mode coupling theories (MCT) [29] have contributed greatly to discussions of the dynamics of supercooled liquids and the liquid-glass transition for molecular systems, predicting power law divergences in the relaxation times and extracting the glass transition through analyses of bifurcations in the self-consistent long-time solutions of the MCT equations. The equilibrium static structure factor is required as input, along with approximations for the coupling factors that appear in the general formulation. With the Verlet-Weiss correction to the Percus-Yevick structure factor for hard spheres, the simplest formulation, known as ideal mode coupling, predicts a glass transition at $\phi_g=0.525$, which is much too low. This is taken to indicate that the theory exaggerates the ''caging'' effect through which neighbors constrain particle motion. If the volume fraction is rescaled as $\phi=(\phi_g/0.525)\phi^{\rm MCT}$ with ϕ_g as an adjustable parameter, the MCT predicts the residual, i.e., nondecaying, part of the dynamic structure factor beyond the glass transition in nearly quantitative agreement with dynamic light scattering measurements from dispersions of colloidal hard spheres. The volume fraction and wave number dependence of the decay of the dynamic structure factor below and above the glass transition are also captured qualitatively. The low-shear viscosity is predicted to diverge at the glass transition as $\Delta\eta_o\propto(\phi_g-\phi)^{-2.59}$. An extended formulation of mode coupling theory exists in part, in an attempt to incorporate ''hopping events (that) appear because phonons kick particles over barriers'' [30]. This is expected to allow the dynamic structure factor to relax completely at longer times, which should also produce a finite low-shear viscosity up to random close packing, but results are very limited to date.

The direct application of the molecular theory to colloidal dispersions is not entirely satisfying, since the complete neglect of hydrodynamic interactions precludes a quantitative description of the dynamics. Also, the high-frequency responses retain the divergence characteristic of underdamped molecular systems. Recently Nägele, Bergenholtz, and coworkers [19,31,32] have developed several strategies for assessing the validity of the approach for colloidal dispersions and incorporating hydrodynamic interactions. These include careful comparisons of predictions (a) in the dilute limit with exact solutions from Smoluchoski formulations without hydrodynamic interactions and (b) at higher concentrations with results from Brownian dynamics simulations. In the di-

lute limit the predictions from MCT are semi-quantitative, i.e., differing at $O(1)$ in numerical prefactors. At higher concentrations the dynamics are reproduced accurately in a broad sense, if $\phi_g = 0.62$ is chosen to fit values for the long-time self-diffusion coefficient from simulations up to $\phi = 0.50$. By adapting the rescaling described above to account for hydrodynamic interactions, they obtained good agreement with low-shear viscosities measured by Segré *et al.* [13], for $\phi \leqslant 0.49$ and relaxation times from earlier viscoelastic measurements by van der Werff *et al.* [33]. The full viscosity then diverges at ϕ_g as $\eta_o \propto (\phi_g - \phi)^{-2.59}$ with some enhancement from the weak logarithmic divergence in the high-frequency viscosity (5) at ϕ_m.

The extant data for the low-shear viscosity for colloidal hard spheres extends through the equilibrium fluid phase into the metastable regime. Most of the recent data for PMMA hard spheres lie below the freezing transition, which is 20–25% below the divergence [8,13]. The older data for silica dispersions in cyclohexane and ethylene glycol–glycerol mixtures include sets that reach beyond 0.60 but suffer to varying extent from polydispersity, which reduces the magnitude of the viscosity [17], and an extrapolation to the low-shear limit [13] and significant scatter, which introduce uncertainty into estimates of the maximum packing fraction. Thus, approximate theories that only differ significantly in the vicinity of the divergence, such as those described above, are difficult to distinguish and the volume fraction at the divergence remains uncertain.

In the background is the current ferment about the nature and existence of the hard-sphere glass transition. Recent computer simulations find no thermodynamic glass transition between ϕ_f and ϕ_m [28], in contrast to a number of earlier efforts. Careful dynamic light scattering measurements confirm at least semiquantitatively the mode coupling predictions for the residual or nondecaying portion of the dynamic structure factor and nonergodicity parameters [34]. Very recent studies with confocal microscopy detect dynamic heterogeneities and quantify non-Gaussian aspects of diffusion processes and estimate long-time self-diffusion coefficients [35,36]. These distinguish compact clusters of slow particles from tenuous fractal domains of fast particles and set $\phi_g = 0.58 \pm 0.01$ from the transition in the non-Gaussian response and the size of the compact clusters. On the other hand, the population of fast particles and the finite lifetimes of the compact slow domains seem to translate into long-time self-diffusion coefficients that remain finite beyond the glass transition. Thus a consensus may be emerging that the heterogeneity and nonergodic nature of the dynamics at intermediate times reflect a dynamic glass transition, yet motion continues on longer time scales as reflected by finite long-time self-diffusion coefficients and, presumably, low-shear viscosities.

III. EXPERIMENT

The PMMA-PHSA, poly(methyl methacrylate)-poly(hydroxy stearic acid), particles were synthesized by Ottewill and his group at Bristol University [4] with average core diameters of 518 and 640 nm determined by transmission electron microscopy (TEM). The particles (bulk refractive index $n = 1.491$) were dispersed in two different solvents: 1,2,3,4-*cis/trans*-decahydronapthalene (decalin, $n = 1.4750$), which produced an opaque whitish dispersion, and a mixture of *cis/tran*-decalin and 1,2,3,4-tetrahydronapthalene (tetralin, $n = 1.5410$) that nearly matched the refractive index of the swollen PMMA particles. We convert the weight concentration to effective hard-sphere volume fraction by measuring the densities and refractive indices to determine the free volume and swelling of the particle in each solvent and then constructing an experimental phase diagram from a series of samples with different concentrations. On that basis the scale factor between the mass concentration and the hard-sphere volume fraction is chosen such that $\phi = 0.505$ (accounting for 5% polydispersity) for the mass fraction at which crystals appear. For the unswollen decalin particles this sets the PHSA layer thickness as $L = 15.1 \pm 1.5$ nm and the melting transition at $\phi = 0.552 \pm 0.005$. The melting transition in the mixture occurs at $\phi = 0.544 \pm 0.008$, so both lie almost within experimental error of the theoretical value of 0.555 for 5% polydisperse hard spheres.

The radii of bare silica spheres, courtesy of Nissan Chemical Corp., Tokyo, were determined as 244 ± 10 nm by TEM and dynamic light scattering. The spheres ($n = 1.4583$) were dispersed in a refractive index matching mixture of ethylene glycol ($n = 1.4334$) and glycerol ($n = 1.4752$), which was demonstrated previously to produce hard-sphere behavior [5]. A slight charge on the particles was suppressed by adding 0.054 M KCl in the suspension to reduce the Debye screening length to $\kappa^{-1} = 0.1$ nm. These bare silica spheres remain stable in the index-matching mixture in the absence of electrostatic repulsion, suggesting that hydration of the surfaces by the ethylene glycol suffices to negate the weak dispersion attraction. The viscosity of the solvent is very high, e.g., $\mu(20\,^\circ\mathrm{C}) = 190$ mPa s, $\mu(25\,^\circ\mathrm{C}) = 138$ mPa s, and $\mu(30\,^\circ\mathrm{C}) = 102$ mPa s, and crystallization was not noticeable in two years. They do crystallize, however, when dispersed in formamide, which has a low viscosity and may also induce charges. The initial aqueous dispersions with $\phi \sim 0.20$ were washed by dilution, centrifuged, and redispersed in distilled water three times to remove impurities and possibly smaller particles. Three washes with ethylene glycol then removed the water and three washes with the index-matching mixture balanced the solvent. Finally, these suspensions were centrifuged at 1500g and the supernatant was discarded. The sediment, which was confirmed to have a volume fraction of $\phi_m = 0.64$, then was diluted with the solvent mixture to prepare separate samples at the desired volume fractions by addition of more solvent.

The critical stress associated with shear thinning for hard-sphere fluids is of order [9] $\sigma_c = kT/a^3 \sim 190$ mPa for $a = 244$ nm, but shifts to lower values for $\phi > 0.5$. The Newtonian low-shear regime is reached at stresses an order of magnitude or more below the critical stress, so a critical issue is ensuring sufficiently low shear stresses. For this reason, we use a Zimm-Crothers viscometer [37] as pictured in Fig. 1. A temperature-controlled static outer cylinder contains the fluid of interest plus a neutrally buoyant rotor bal-

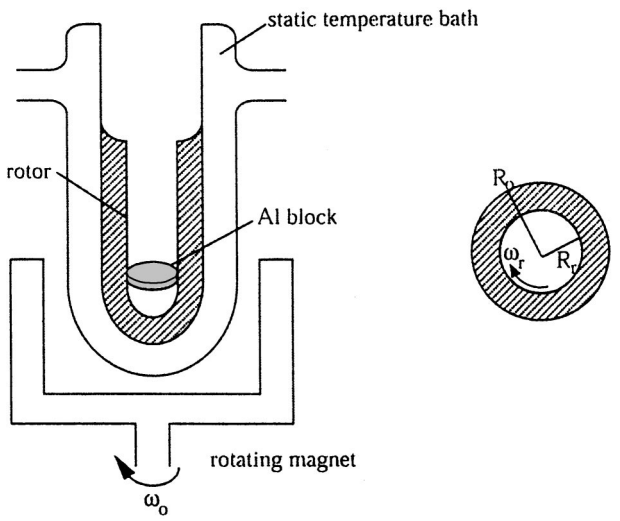

FIG. 1. Zimm viscometer.

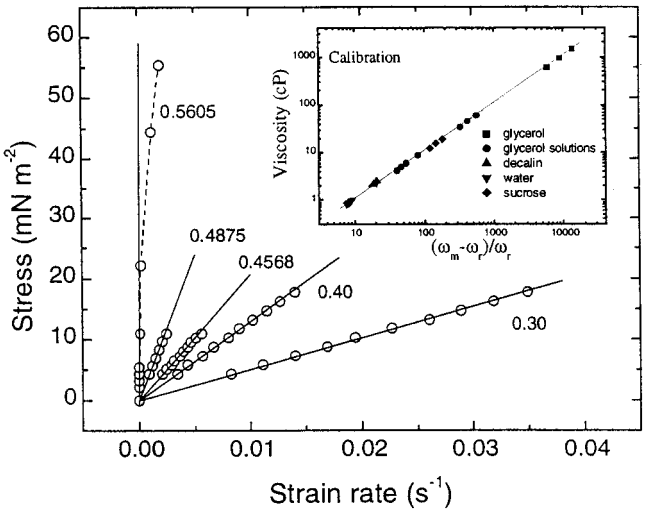

FIG. 2. Shear stress versus shear rate for several concentrated dispersions of bare silica spheres showing the linear region at low shear rates (or stresses) from which the slope yields the low shear viscosity. All these lines extrapolate through the origin within experimental error. At high concentrations ($\phi>0.46$), deviations from linearity indicate the onset of shear thinning. The insert shows the calibration that determines the apparatus constant C.

anced by the addition of aluminum and plastic disks. Surface tension centers the rotor. A constant torque is generated by the interaction of the aluminum disk fixed at the bottom of the rotor with an applied rotating magnetic field. A HP3325A synthesizer/function generator and pulse motor drive the magnet at a constant but adjustable angular velocity ω_m. Thus a constant shear stress is applied to the fluid between the cylinders. The rotation rate of the rotor is detected by reflecting a laser beam from a circular pattern of alternating black and reflective radial strips on the top of the additional plastic disks. As the rotor turns, the beam reflected from a point off the center of the pattern blinks on and off. The beam impinges on a photodiode, whose signal is converted by an analog-to-digital card and analyzed to determine the frequency ω_r. Equating the magnetically induced torque to the viscous torque on the rotor determines the steady shear viscosity as $\eta=C(\omega_m-\omega_r)/\omega_r$ with C the calibration constant that depends on the strength of the magnetic field, the conductivity and size of the aluminum disk, and the radii (R_r and R_o) and surface areas of the rotor and the outer cylinder. We calibrate C by measurements with water, *trans*-decalin, *cis*-decalin, glycerol, and glycerol or sucrose solutions with known viscosities ranging from 1 mPa s to 1.5 Pa s. The average shear stress in the fluid is

$$\sigma=C\frac{4R_o^2R_r^2\ln(R_o/R_r)}{R_o^2-R_r^2}(\omega_m-\omega_r). \tag{14}$$

Because extraneous sources of friction are minimal, stresses as low as 10^{-5} Pa can be applied. Thus, the Newtonian low-shear regimes of the hard-sphere dispersions can be investigated. The inset in Fig. 2 shows the calibration that determines the apparatus constant C, though the relative viscosity η_r is actually independent of the calibration. The main plot in Fig. 2 depicts shear stress versus shear rate for several concentrated dispersions of bare silica spheres. At the higher concentrations the linear regions of the data, whose slopes give the low-shear viscosities, are followed by curvature indicating the beginning of shear thinning.

IV. RESULTS AND DISCUSSION

Our earlier paper [8] compared data for PMMA-PHSA, polystyrene, and silica hard spheres, displaying excellent correlation of the high shear viscosities but considerable scatter for $\phi>0.30$ in the low-shear viscosities. In the studies with polystyrene and silica all the volume fractions were calculated from bulk densities or intrinsic viscosities, some of the data were extrapolated to the low-shear limit, and some suffer from significant polydispersity. These three factors introduce significant uncertainty. The Zimm viscometer eliminates the extrapolation and calibration with respect to an independent measurement at high concentration provides an accurate volume fraction. The hard-sphere freezing transition, as originally argued by Pusey [6], seems most appropriate when crystallization is evident, as for the PMMA-PHSA/decalin-tetralin systems. Random close packing is a suitable alternative for our SiO_2/ethylene glycol–glycerol system and is relatively insensitive to low levels of polydispersity. In the absence of either of these, as for the PMMA-PHSA/mineral oil system [38], the high shear viscosity offers another robust property that reflects the hydrodynamic volume. Figure 3 demonstrates the agreement among data for the PMMA-PHSA and the current silica dispersions to be excellent after these corrections. The two outlying points at high volume fractions correspond to PMMA-PHSA at $\phi>0.494$, in which crystallization may have occurred without being detected.

This new ''master curve'' for the PMMA-PHSA/decalin-tetralin and SiO_2/ethylene glycol–glycerol (SiO_2/EG-Gly) dispersions lies significantly above the previously accepted one, which was based on the polystyrene and SiO_2-C_{18}/cyclohexane systems [39]. The data for SiO_2-C_{18}/cyclohexane obtained by de Kruif are undoubtedly

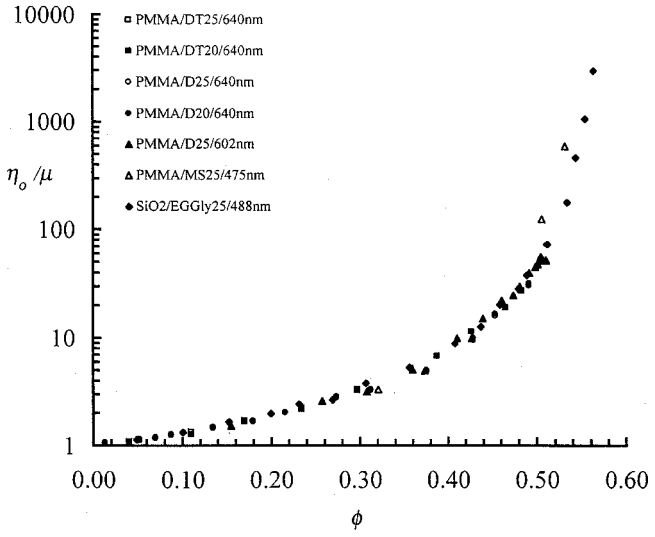

FIG. 3. Relative low shear viscosities as a function of volume fraction for PMMA-PHSA spheres in decalin, decalin-tetralin mixtures, and mineral spirits [8,13,38] and SiO_2 spheres in ethylene glycol-glycerol mixtures from this work.

affected by polydispersity [17] and may also suffer some uncertainty due to the extrapolation to the low-shear limit [13]. The original hard-sphere data for polystyrene from Krieger are difficult to impeach on any grounds other than guilt by association. Nonetheless, the addition of the current SiO_2/EG-Gly data to that for the PMMA-PHSA dispersions constitutes a database in which several important factors have been treated consistently: (1) a high volume fraction reference for the conversion from weight fraction, (2) access to sufficiently low-shear stresses to reach the Newtonian limit, (3) independent evidence of hard-sphere behavior, and (4) minimal effect of polydispersity. Agreement among the various data sets for the equilibrium fluid ($\phi < 0.50$) is excellent, and the data for silica extend the curve well into the metastable fluid regime.

Given these data we now assess the accuracy of the theories described earlier and seek insight into the nature and location of the divergence in the viscosity. Figure 4 superimposes on the data predictions from Stokesian and Brownian dynamics, Smoluchoski, and mode coupling approaches. Clearly for $\phi \leqslant 0.45$ the full Stokesian dynamics simulations, the rescaled mode coupling theory, and the rescaled Smoluchoski theory with the potential of mean force closure reproduce the data quite satisfactorily. Over this range, rescaling of Brownian dynamics simulations without hydrodynamic interactions yields low-shear viscosities that are somewhat low and Brady's rescaling of the dilute limit from the Smoluchoski theory without hydrodynamic interactions falls marginally above the data. However, the real differences appear for $\phi > 0.45$, where many-body thermodynamic interactions become very strong. Here only the rescaled mode coupling theory and the rescaled Brownian dynamics simulations come close. Replotting the theories and the same data, with the two outlying data points eliminated, to highlight the thermodynamic contribution $\Delta\eta_o$ (Fig. 5) provides a more telling comparison. Plotting $\Delta\eta_o$ against $1/(0.64-\phi)$ on log-linear coordinates suggests that the (presumably power law) divergences in the theories and the Brownian dynamics simulations do not capture the apparently exponential divergence in the data.

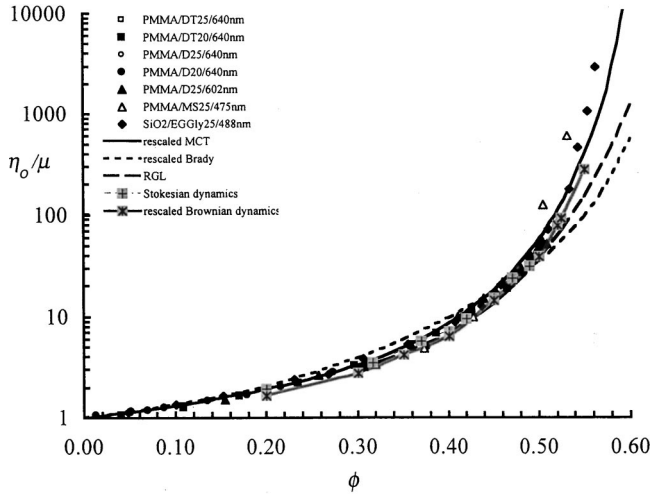

FIG. 4. Comparison of relative low shear rate viscosities with predictions from nonequilibrium theories and simulations. Stokesian dynamics simulations [24] (+), rescaled Brownian dynamics simulations without hydrodynamic interactions [25] (*), rescaled mode coupling theory [19] (—), rescaled Smoluchoski theory with potential of mean force closure [17] (--), and rescaled dilute limit of Smoluchoski theory [20] (— — —).

Motivated by this trend we compare the same data with expectations from the Doolittle and Adam-Gibbs models on slightly different coordinates in Fig. 6. Here, of course, each

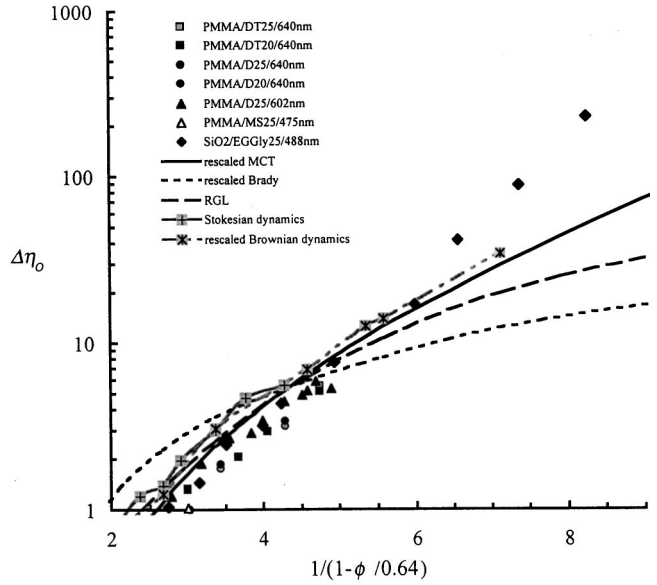

FIG. 5. Comparison of thermodynamic contribution to the low shear viscosities with predictions from nonequilibrium theories and simulations. Stokesian dynamics simulations [24] (+), rescaled Brownian dynamics simulations without hydrodynamic interactions [25] (*), rescaled mode coupling theory [19] (—), rescaled Smoluchoski theory with potential of mean force closure [17] (--), and rescaled dilute limit of Smoluchoski theory [20] (— — —).

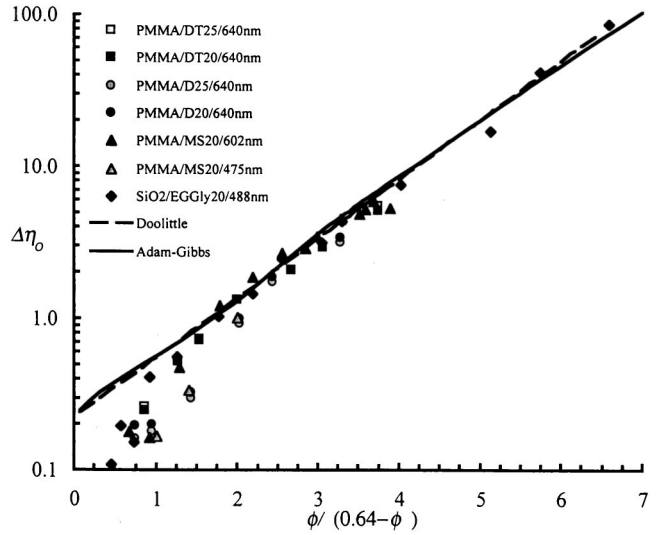

FIG. 6. Comparison of thermodynamic contribution to the viscosity with predictions from phenomenological theories: the Doolittle equation with $C=0.225$ and $\gamma=0.9$ (---) and the Adam-Gibbs equation (—) with $C=0.17$ and $\ln 2\delta\mu/kT=0.9$.

theory contains two adjustable parameters, the preexponential factors C and the coefficients γ and $\delta\mu/kT$ in the exponents. The data are fit remarkably well for $\phi>0.3$, and the two curves essentially collapse, with

	C	γ	$\delta\mu/kT$
Doolittle	0.225	0.9	
Adam-Gibbs	0.17		1.30

Indeed, $\phi>0.3$ is exactly where pair interaction, i.e., dilute, theories begin to fail and many-body interactions become important. The salient feature of both models is an exponential dependence of the low-shear viscosity on volume fraction with the common limiting form

$$\Delta\eta_o \cong 0.2\exp[0.6/(0.64-\phi)]. \tag{15}$$

The collapse is not exact because the functional forms in the exponents differ and the Doolittle equation actually diverges at $\phi=0.64$, while the results from simulations [28] used to evaluate the Adams-Gibbs model set the divergence at $\phi=0.644$. If one plots $1/\ln\Delta\eta_o$ vs ϕ without assuming a divergence at 0.64, the data follow

$$\Delta\eta_o \cong 1.47\exp[0.116/(0.625-\phi)]. \tag{16}$$

Since the extrapolation from the measurement at $\phi=0.562$ to the divergence at 0.64 is rather long, one or more additional data points, particularly at or beyond the expected glass transition near 0.58, would establish the divergence more convincingly. Indeed we have tried. The difficulty is easily illustrated, since the critical stress characterizing shear thinning falls linearly toward zero at random close packing roughly as $a^3\sigma_c/kT\cong 3(0.64-\phi)$ [39]. Combining this with the asymptotic form (15) for $\Delta\eta_o$ and (5) for η'_∞ permits an estimate for the time required to achieve unit strain at a stress an order of magnitude smaller than the critical value, as required to assure Newtonian behavior. The times are prohibitive for the SiO_2/ethylene glycol–glycerol system, i.e., roughly 35 days at $\phi=0.58$ and 350 days at $\phi=0.59$.

This correlation indicates that the low-shear viscosity for hard spheres diverges exponentially in the vicinity of $\phi=0.64$, rather than at a hard-sphere glass transition expected to lie significantly below random close packing. Careful computer simulations establish the absence of a thermodynamic glass transition for hard spheres [28], but dynamic light scattering [34] and confocal microscopy [35] identify a transition in the dynamics at $\phi\cong 0.58$. On the other hand, the confocal experiments still detect motion at the longest times observed beyond 0.58 [34,35] and, in microgravity, dispersions of PMMA-PHSA spheres at volume fractions up to 0.64 crystallize in two weeks [40,41]. Thus evidence exists that the dynamics are not fully arrested below random close packing.

This is not the first recognition of conformity of large increases in viscosity near close packing with the Doolittle and Adam-Gibbs equations. Woodcock and Angell [42] simulated hard-sphere liquids by molecular dynamics and correlated the inverse of the self-diffusion coefficient for $\phi>0.50$ with the Doolittle equation with $\phi_m=0.637$ and γ close to unity. For SiO_2-C_{18} spheres in dodecane Marshall and Zukoski [43] found the low-shear viscosity for the metastable fluid to conform quite well to the Doolittle equation with $\phi_m=0.64$, though the data contained considerable scatter. For glycerol, one of the most widely studied glass-forming liquids, Herbst, Cook, and King [44] measured the density dependence of the viscosity, close to glass transition temperature, at pressures up to 3 GPa. Free volume theory, which ascribes an incompressible hard-sphere volume to the molecules, correlates the data well over the entire pressure range and, by extrapolation to the glass transition, over 12 orders of magnitude in viscosity.

However, Woodcock and Angell [42] point out that the success of the Doolittle equation for hard spheres should not be construed as a vindication of the underlying models. Rather, the free volume theories could arrive at the right expression from a model that oversimplifies the actual transport mechanism. Indeed, the similarity of the functional form to that from the Adam-Gibbs theory supports this assertation. Surely, the recent findings described above for heterogeneous structure in metastable fluids [35,36] offer different and, perhaps, more sound ways of thinking about the glass transition, which may be more consistent with the cooperative rearrangements envisioned by the Adam-Gibbs approach.

In summary, precise data for the low-shear viscosity as a function of volume fraction on two model colloidal hard-sphere dispersions, PMMA-PHSA, and bare SiO_2 spheres,

indicate a viscous fluid state, presumably metastable, up to random close packing. Smoluchoski and mode coupling theories fail to capture the divergence, whereas the Doolittle and Adam-Gibbs equations offer exponential forms that correlate the data well, given two $O(1)$ adjustable parameters. The available Stokesian dynamics simulations also conform to the data but do not extend to sufficiently high volume fractions.

ACKNOWLEDGMENT

This research was supported by the NASA Microgravity Sciences Program.

[1] W. G. Hoover and F. H. Ree, J. Chem. Phys. **49**, 3609 (1968).
[2] L. V. Woodcock, Ann. N.Y. Acad. Sci. **37**, 274 (1981).
[3] J. P. Hansen and L. R. McDonald, *Theory of Simple Liquids* (Academic, New York, 1986).
[4] L. Antl, J. W. Goodwin, R. D. Hill, R. H. Ottewill, S. M. Owens, and S. Papworth, Colloids Surf. **17**, 67 (1986).
[5] T. Shikata and D. S. Pearson, J. Rheol. **38**, 601 (1994).
[6] P. N. Pusey and W. van Megen, Nature (London) **320**, 340 (1986).
[7] P. N. Pusey, in *Liquids, Freezing, and the Glass Transition*, edited by J. P. Hansen, D. Levesque, and J. Zinn-Justin (Elsevier, Amsterdam, 1991), Chap. 10, pp. 763–941.
[8] S.-E. Phan, W. B. Russel, Z. Cheng, J. Zhu, P. M. Chaikin, J. H. Dunsmuir, and R. H. Ottewill, Phys. Rev. E **54**, 6633 (1996).
[9] I. M. Krieger, Adv. Colloid Interface Sci. **3**, 111 (1972).
[10] C. G. de Kruif, E. M. F. van Iersel, A. Vrij, and W. B. Russel, J. Chem. Phys. **83**, 4717 (1986).
[11] J. C. van der Werff and C. G. de Kruif, J. Rheol. **33**, 421 (1989).
[12] P. N. Segré, S. P. Meeker, P. N. Pusey, and W. C. K. Poon, Phys. Rev. Lett. **75**, 958 (1995).
[13] P. N. Pusey, P. N. Segré, O. P. Behrend, S. P. Meeker, and W. C. K. Poon, Physica A **235**, 1 (1997).
[14] T. Palberg, J. Phys.: Condens. Matter **11**, R323 (1999).
[15] Z. Cheng, J. Zhu, W. B. Russel, and P. M. Chaikin, Phys. Rev. Lett. **85**, 1460 (2000).
[16] P. G. Debenedetti, *Metastable Liquids: Concepts and Principles*, (Princeton University Press, Princeton, NJ, 1996).
[17] R. A. Lionberger and W. B. Russel, Adv. Chem. Phys. **111**, 399 (2001).
[18] G. K. Batchelor, J. Fluid Mech. **83**, 97 (1977).
[19] A. J. Banchio, G. Nägele, and J. Bergenholtz, J. Chem. Phys. **111**, 8721 (1999).
[20] J. F. Brady, J. Chem. Phys. **99**, 567 (1993).
[21] A. Sierou and J. F. Brady, J. Fluid Mech. **448**, 115 (2001).
[22] N. J. Wagner, J. Non-Newtonian Fluid Mech. **96**, 177 (2001).
[23] J. F. Brady, Annu. Rev. Fluid Mech. **20**, 111 (1988).
[24] D. R. Foss and J. F. Brady, J. Fluid Mech. **407**, 167 (2000).
[25] D. R. Foss and J. F. Brady, J. Rheol. **44**, 629 (2000).
[26] H. Z. Cummins, G. Li, Y. H. Hwang, G. Q. Shen, W. M. Du, J. Hernandez, and N. J. Tao, Z. Phys. B: Condens. Matter **103**, 501 (1997).
[27] M. H. Cohen and D. J. Turnbull, J. Chem. Phys. **31**, 1164 (1959); D. J. Turnbull and M. H. Cohen, *ibid.* **34**, 120 (1961); **52**, 3038 (1970).
[28] M. D. Rintoul and S. Torquato, J. Chem. Phys. **105**, 9258 (1996).
[29] W. Götze, in *Liquids, Freezing, and the Glass Transition*, edited by J. P. Hansen, D. Levesque, and J. Zinn-Justin (Elsevier, Amsterdam, 1991), Chap. 5, pp. 289–503.
[30] W. Götze and L. Sjögren, Transp. Theory Stat. Phys. **24**, 801 (1995).
[31] G. Nägele and J. Bergenholtz, J. Chem. Phys. **108**, 9893 (1998).
[32] A. J. Banchio, J. Bergenholtz, and G. Nägele, Phys. Rev. Lett. **82**, 1792 (1999).
[33] J. C. van der Werff, C. G. de Kruif, C. Blom, and J. Mellema, Phys. Rev. A **39**, 795 (1989).
[34] W. van Megen and S. M. Underwood, Phys. Rev. Lett. **70**, 2766 (1993).
[35] E. R. Weeks, J. C. Crocker, A. C. Levitt, A. Schofield, and D. A. Weitz, Science **287**, 627 (2000).
[36] W. K. Kegel and A. van Blaaderen, Science **287**, 290 (2000).
[37] B. H. Zimm and D. M. Crothers, Proc. Natl. Acad. Sci. U.S.A. **48**, 905 (1962).
[38] J. Mewis, W. J. Frith, T. A. Strivens, and W. B. Russel, AIChE J. **35**, 415 (1989).
[39] W. B. Russel, D. A. Saville, and W. R. Showalter, *Colloidal Dispersions* (Cambridge University Press, Cambridge, England, 1989).
[40] J. Zhu, M. Li, R. Rogers, W. V. Meyer, R. H. Ottewill, W. B. Russel, and P. M. Chaikin, Nature (London) **387**, 883 (1997).
[41] Z. Cheng, J. Zhu, W. V. Meyer, R. Rogers, R. H. Ottewill, W. B. Russel, and P. M. Chaikin, Mater. Des. **22**, 529 (2001).
[42] L. V. Woodcock and C. A. Angell, Phys. Rev. Lett. **47**, 1129 (1981).
[43] L. Marshall and C. F. Zukoski, J. Chem. Phys. **94**, 1164 (1990).
[44] C. A. Herbst, R. L. Cook, and H. E. King, Jr., Nature (London) **361**, 518 (1003).